JOURNAL OF MATERIALS SCIENCE 27 (1992) 2279–2290

Plane-stress essential work of ductile fracture for polycarbonate

C. A. PATON, S. HASHEMI
London School of Polymer Technology, The Polytechnic of North London, Holloway Road, London N7 8DB, UK

The effect of specimen geometry, specimen size and the specimen orientation on the essential work of fracture for polycarbonate is investigated. Two different test geometries, namely the single-edge notched tension and double-edge notched tension specimens, are used to evaluate the essential work of fracture for crack propagation. It is shown that the specific essential work of fracture for crack propagation, w_e, is independent of the test piece geometries and the size of the test piece. It seems that for a given sheet thickness, w_e is a fundamental material property being independent of the specimen geometry and size. The value of w_e does change with the orientation of the initial notch with respect to the melt flow direction. The straight-line relationships between the total specific work of fracture, w_f, and ligament length, L, breaks down when the ligament length to specimen thickness ratio is less than about three, because the fracture data fall in the plane stress–plane strain transition region. A plane strain specific essential work of fracture, w_{1e}, was obtained by extrapolating the best regression line of the data to a zero ligament. For the initial notch in the melt flow direction, values for w_e and w_{1e} were approximately 28 and 3 kJ m^{-2}, respectively. The specific essential work of initiation, w_i, was about 4.3 kJ m^{-2}. J_R curves (J–Δa curves) were also obtained and it is shown that the intercept and the slope of the J_R curve, i.e. J_c and dJ/da, are related to w_e and the slope of the w_f versus ligament plot.

1. Introduction

The theory of linear elastic fracture mechanics (LEFM) deals with fractures occurring at nominal stresses that are well below the uniaxial yield stress of the material. Under this condition, plastic flow at the tip of the crack is intimately associated with the fracture process which is brittle in nature. A single fracture parameter such as the critical stress intensity factor, K_c, or the critical strain energy release rate, G_c, is sufficient to characterize this fracture at its critical condition. However, because fracture processes are controlled by the crack tip stresses and strains, and the states of triaxial stresses near the crack tip are influenced greatly by the specimen size, the fracture parameter, K_c, is expected to vary with the size of the specimen used. The material parameter is therefore best characterized when plane-strain conditions exist. To achieve this state of stress the specimen size must exceed some multiple of the plastic zone size at the tip of the crack. This limitation on the specimen size forms the basis of the minimum test-piece size requirements of the ASTM E-399 standard for valid determination of K_c (K_{Ic}) which is given by [1]

$$a, B, W - a \geqslant 2.5\left(\frac{K_c}{\sigma_y}\right)^2 \quad (1)$$

where B and W are the specimen thickness and width, respectively, and σ_y is the uniaxial yield stress of the material. Such limiting size requirement for the use of LEFM in determining K_c in relatively brittle materials presents no practical difficulties and determination of K_c can be carried out on reasonably sized specimens (e.g. [2, 3]). However, the restriction of the small-scale yielding places a severe limitation on the application of LEFM in characterizing the fracture toughness in ductile materials, where the plastic zone sizes are not small with respect to the dimensions of the specimen and therefore the crack tip stress field can no longer be characterized by a K_c value.

For ductile materials, two approaches have been used in order to characterize the fracture behaviour. The most widely used parameter for characterizing fracture in ductile materials is that proposed by Rice [4] and is called J-integral, which is a path independent line integral expressed in terms of energy as

$$J = -\frac{1}{B}\frac{dU}{da} \quad (2)$$

where U is the potential energy of the loaded body. The critical value of the J-integral is called J_c. For fracture to be characterized by J_c, a specimen must meet a certain size constraint in order to generate a plane-strain constraint along the crack front. To achieve this stress state, all specimen dimensions must exceed some multiple of J_c/σ_y. According to ASTM [5, 6], the plane-strain value of J_c (i.e. J_{Ic}) may be

0022–2461

determined whenever

$$B, W - a, W \geqslant 25\left(\frac{J_c}{\sigma_y}\right) \quad (3)$$

It has been demonstrated by several investigators [7–12] that polymers can be characterized by the J-integral approach.

Another approach used to characterize the fracture behaviour of ductile materials is called the Essential Work which was originally proposed by Broberg [13]. In this method, the total work of fracture is considered to be made of two components: one associated with plastic work and considered to be non-essential and the other associated with initiation of instability and regarded as essential work of fracture. The later may be regarded as a material property characterizing fracture under plane-stress conditions. Following the Broberg idea, it was proposed [14–17] that the total specific work of fracture or the work of fracture per unit ligament area may be written as

$$w_f = w_e + \beta L w_p \quad (4)$$

where w_f is total specific work of fracture, w_e is the specific essential work of fracture, w_p is the specific plastic work of fracture, L is the ligament length and β is a shape factor which describes the size of the plastic zone. According to the above equation, a straight-line relationship exists between the specific work of fracture and the ligament length and w_e can be obtained when L is extrapolated to zero. It has been demonstrated by Mai and Cottrell [15] that plane-stress ductile fracture in polymers can be characterized by the fracture parameter, w_e.

This paper reports the results of an experimental investigation on the essential work of fracture for injection-moulded polycarbonate sheets of nominal thickness 1.7 mm with initial notches normal, parallel and at 45° to the direction of the flow of material. The effect of specimen geometry, specimen size, notch orientation and the notch sharpness on the specific essential work of fracture were also investigated. A comparison is also made with the J-integral technique.

2. Experimental procedure

Polycarbonate, trade name LEXAN 943, was used in the present studies. The polycarbonate samples were in the form of 1.7 mm thick injection-moulded plaques of nominal dimensions 90 mm by 90 mm. Specimens were cut from each plaque either perpendicular, parallel or at 45° to the direction of the melt flow as shown in Fig. 1. The measured value of the Young's modulus was about 2 GPa and the yield stress was about 60 MPa (these values were measured at 23 °C and at a constant crosshead rate of 1 mm min^{-1}). The monotonic tensile tests did not show any differences between either the yield stresses or the elastic moduli of samples that are perpendicular, parallel or at 45° to the direction of flow of material.

For fracture studies, the initial notches were prepared by first forming saw cut slots which were then sharpened with a razor blade. The razor blade was mounted on a laboratory attachment so that penetration could be controlled carefully. The fresh edge of a razor was then pushed through the material slowly to a depth of about 1 mm. The notch length measurement was done using a travelling microscope.

The majority of the tests were carried out using single-edge notched tension specimens (SENT), but double-edge notched tension (DENT) tests were also performed (see Fig. 2) to investigate whether the results were geometry dependent. Utilization of specimens of differing overall dimensions was also made, to

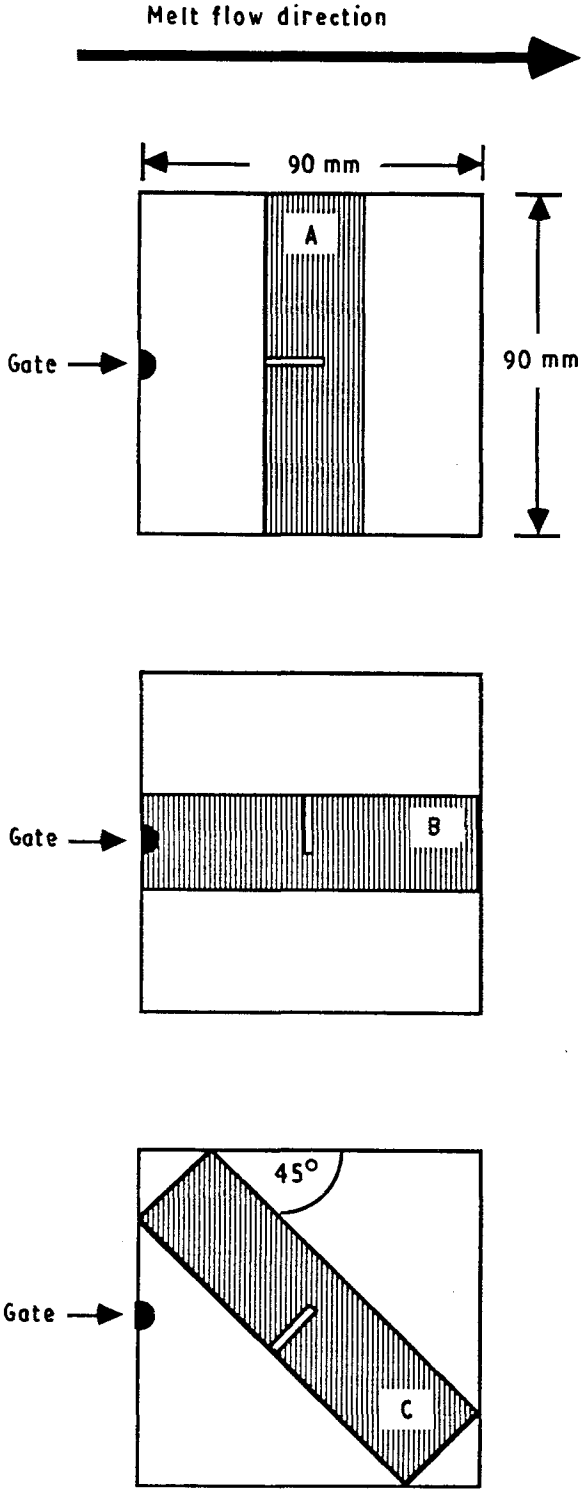

Figure 1 Specimen orientations A–C with respect to the melt flow direction. A, crack is in the melt flow direction. B, crack is at 90° to the melt flow direction. C, crack is at 45° to the melt flow direction.

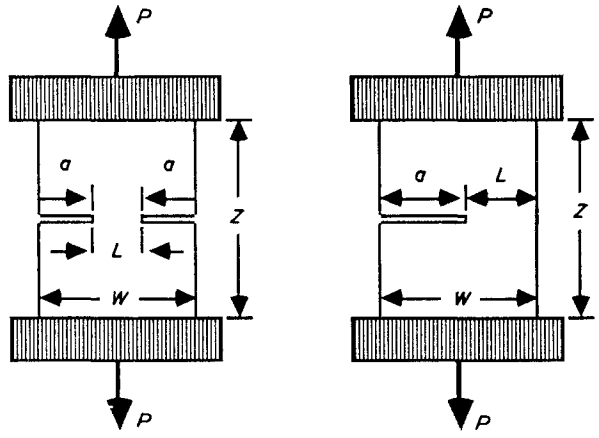

Figure 2 Specimen configurations for determination of specific essential fracture work.

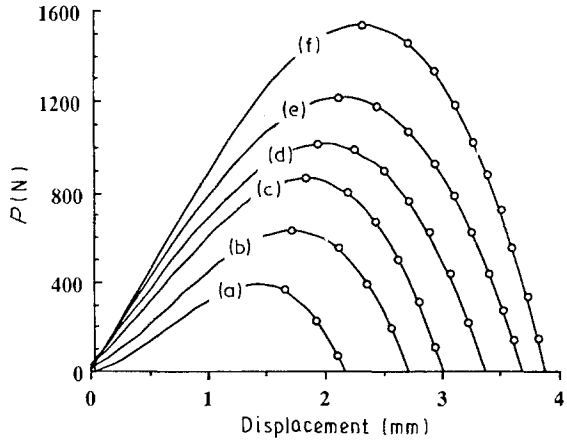

Figure 3 Load–displacement curves for fractures in SENT polycarbonate specimens with varying ligament lengths. Open circles mark every 2 mm crack growth (the first open circle is for the first 2 mm growth). Crack growth is in direction of the melt flow. L (mm): (a) 7.030, (b) 10.93, (c) 13.35, (d) 17.02, (e) 19.73, (f) 22.22.

investigate any significant size effects on the measured values.

All the specimens were fractured at room temperature on an Instron testing machine at a constant crosshead rate of 1 mm min^{-1}. A load–displacement trace for each specimen was recorded. Tests were performed with initial crack lengths varying from 0.1–0.8 of the sample width, W, and the ligament was marked in 2 mm intervals. As the crack passed each marker, the load–displacement record was blipped so that, finally, a series of load–displacement diagrams with crack length marks on them was obtained. Typical load–displacement diagrams for various ligament sizes are shown in Fig. 3 and clearly under the testing conditions employed here this grade of polycarbonate did not fail in a brittle manner. All of the specimens exhibited ductile failure with gross yielding and necking so that no K_c criterion could be considered. The presence of the plane stress deformation was apparent by the contraction of the specimen surfaces. Slow crack growth was observed in all the specimens and the onset of slow crack growth (crack initiation) always occurred after crack-tip blunting as shown in Fig. 4, but in all cases prior to reaching the maximum load, thus indicating cracking at the notch tip prior to

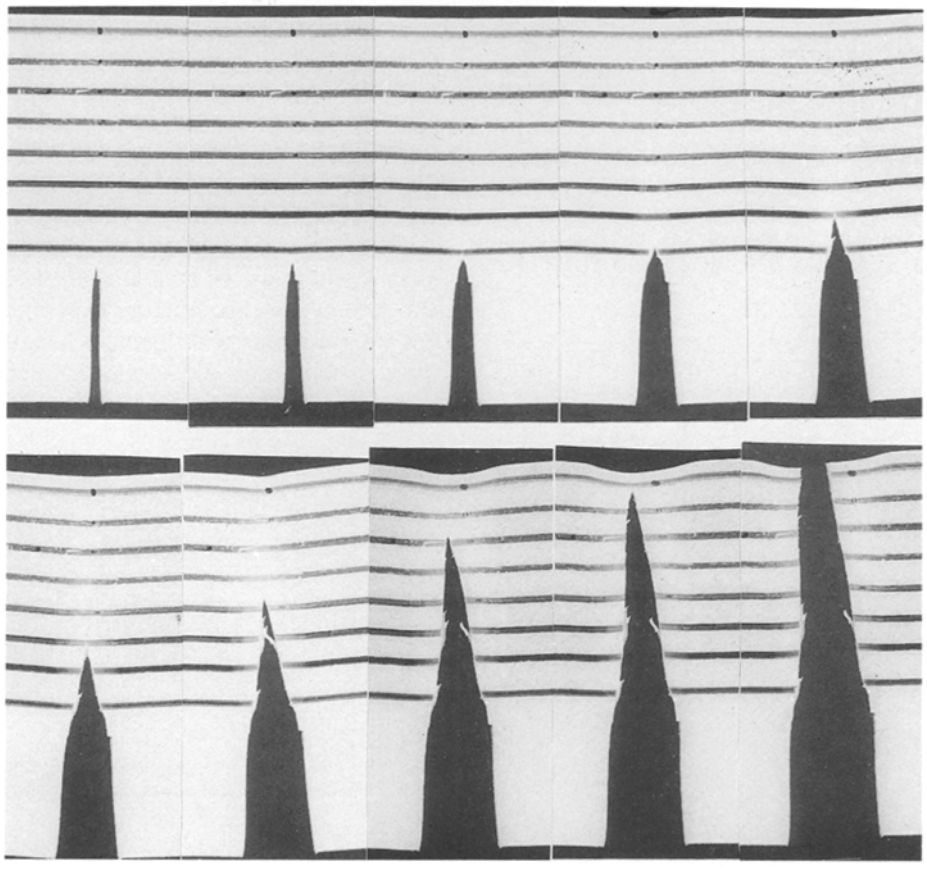

Figure 4 Single-edge notch specimen tearing under load.

gross ligament yielding. Slow crack growth continued beyond the maximum load by ductile tearing under plane stress conditions as the load dropped towards zero. When the maximum load was plotted against ligament length the results behaved linearly for ligament lengths greater than about 20 mm (i.e. $a/W < 0.2$) as shown in Fig. 5. However, for ligament lengths smaller than 20 mm the line did not pass through the origin indicating no true geometric similarity and therefore confirms the visual observation that the crack initiation occurs before the maximum load is reached.

3. The essential work of fracture and the experimental results

It has been suggested by Broberg [13] that the non-elastic region at the tip of a crack may be divided into an end region, where the fracture process takes place, and an outer region, where screening plastic deformation is necessary to accommodate the large strains in the end region as shown in Fig. 6. Following Broberg's ideas it should be possible to characterize ductile fracture by partitioning the work of fracture into two parts – work that goes into the end region and the work that goes into the outer region. The end region work initiates the crack and is termed the essential work of fracture, W_e, and the outer region work which is responsible for plastic deformation is termed W_p. The total fracture work is therefore written as

$$W_f = W_e + W_p \tag{5}$$

The essential work of fracture is proportional to the ligament length, L. The non-essential work in the rest of the plastic region is proportional to L^2, i.e. we may write

$$W_f = LBw_e + L^2B\beta w_p \tag{6}$$

where w_e is the specific essential work of fracture, defined as essential work in the specimen with a unit thickness, B, and unit ligament length, L, and w_p is the non-essential work, defined as the plastic work in a specimen with unit thickness, B, and unit ligament length, L. β is a shape factor depending on the geometry of the plastic zone. Therefore, the total specific fracture work, w_f, according to Equation 6 may be defined as

$$w_f = \frac{W_f}{LB} = w_e + \beta w_p L \tag{7}$$

The above equation suggests that plotting the specific work of fracture, w_f, as a function of ligament length, L, should yield a straight line. The intercept of the line will give the specific essential work of fracture, w_e, and the slope of the line gives a measure of βw_p which is non-essential specific work term as shown in Fig. 7.

For Equation 7 to yield a straight-line relationship between w_e and L, the specimen size must be chosen such that w_e, w_p and β are all independent of the ligament length. To achieve this specimen size must be such that the state of pure plane-stress always exists in the specimen, because only under pure plane-stress state w_e, w_p and β are all constants.

To generate a state of pure plane-stress, the ligament length must be greater than specimen thickness and because of this, fracture experiments are carried out on specimens with ligament lengths greater than three to five times the specimen thickness [15]. For samples with ligament lengths smaller than $3B$–$5B$

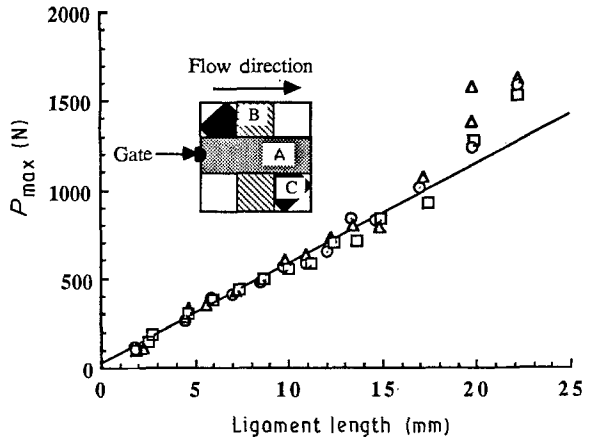

Figure 5 Maximum load in the SENT specimens with dimensions $W = 25$ mm and $Z = 58$ mm. The crack orientation for A (□) is perpendicular to the melt flow direction, for B (○) is in the melt flow direction and for C (△) is at 45° to the melt flow direction. The line drawn is the best fit through the data with equation $P_{max} = 18.57 + 56.14\ L$ ($r = 0.983$).

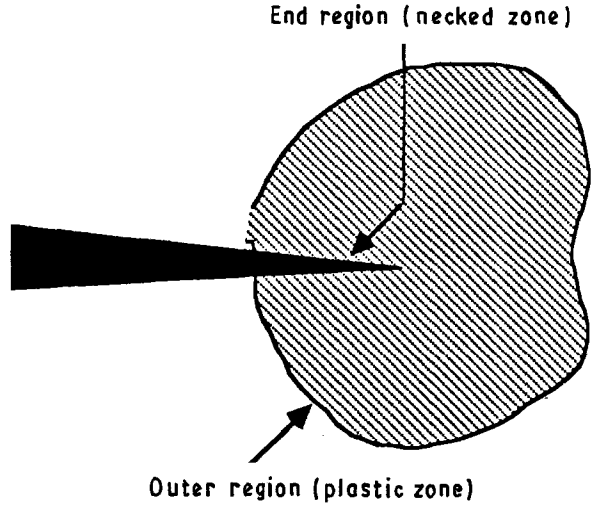

Figure 6 Crack tip deformation zone in a ductile material.

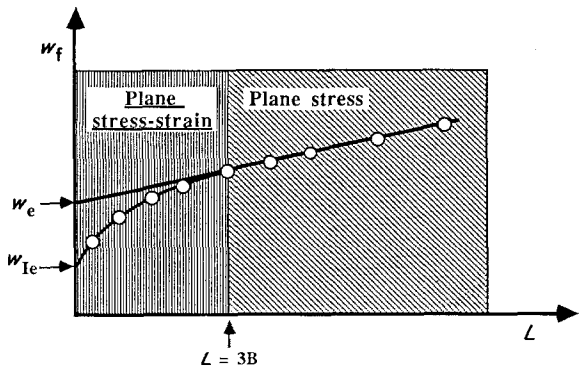

Figure 7 Schematic plot of total specific fracture work versus ligament length showing plane stress and plane strain regions.

there is a fracture transition from plane-stress to plane-strain (i.e. plane-stress/plane-strain) and when ligament length approaches zero, a fully plane-strain fracture is obtained.

In the mixed-mode stress state because of the increasing plastic flow constraint with decreasing ligament length, w_f decreases as shown schematically in Fig. 7. A linear relationship between w_f and L does not necessarily occur. It is possible to determine the plane-strain specific essential work of fracture, w_{Ie}, by either a linear extrapolation of the mixed-mode data to zero ligament length or by fitting a parabolic-shaped curve to the experimental data or using the more elaborate scheme as proposed by Saleemi and Narin [18].

Another factor to be considered is that the size of the plastic zone must not be disturbed by the edge effects, which often arise if the ligament length is not small compared to the total sample width, W. To prevent edge effects it is recommended [14] to keep the ligament length smaller than one-third of the sample width (i.e. $L < W/3$) particularly when double-edge notched tension specimens are used.

3.1. Experimental results on the injection-moulded polycarbonate plaques

3.1.1. Effect of specimen orientation on the plane-stress essential work of fracture

From the areas under load–displacement diagrams, the specific work of fracture, w_f, was calculated and plotted against the ligament length, L. Results obtained for SENT specimens with nominal dimensions $W = 25$ mm and $Z = 58$ mm, and with initial notches parallel, perpendicular and at 45° to the melt-flow direction are shown in Figs 8–10, respectively. It is obvious from the figures that the data for specimens with ligament lengths greater than about 5 mm are well described by Equation 7. From the results presented in Figs 8–10 several observations can be made.

Firstly, as shown in Fig. 8, for a given notch orientation (e.g. parallel to the melt flow direction) the distance from which specimens are cut from the plaque relative to the gate have no significant effect on the essential work of fracture, w_e, or the specific non-essential work term fracture, βw_p. All the data lie on a straight line which can be back-extrapolated to give the plane stress essential work of fracture of about 27.25 kJ m^{-2}. Table I gives values for w_e and βw_p for the three-specimen position as analysed separately and clearly there is no significant difference between the values.

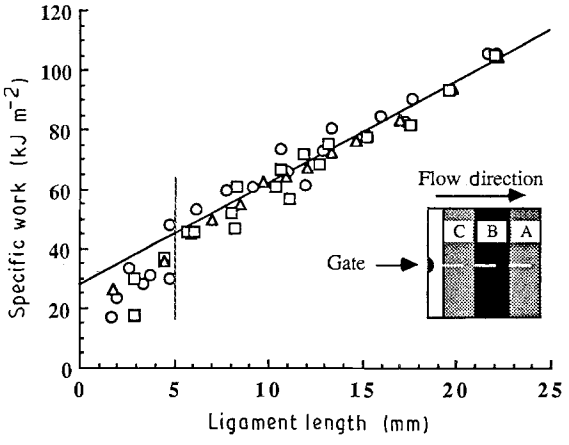

Figure 8 The total specific work of fracture, w_f, for SENT specimens as a function of ligament length L for cracks growing parallel to the flow direction. Specimens are cut at positions (○) A, (△) B, (□) C within the plaques as shown in the figure. The line is a best fit through all the plane-stress data or the data for $L \geqslant 3B$ (i.e. $L \geqslant 5$ mm).

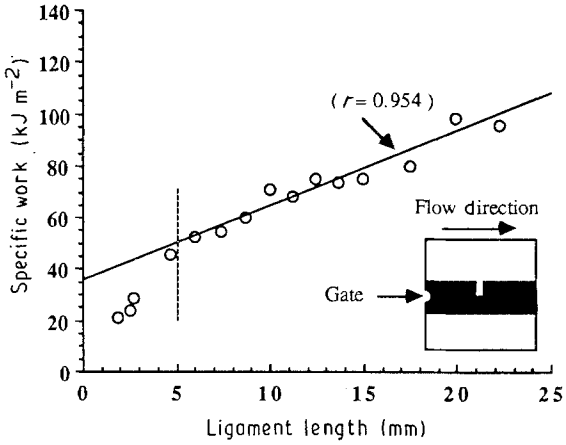

Figure 9 The total specific work of fracture, w_f, for SENT specimens as a function of ligament length, L, for cracks growing in the direction perpendicular to the melt flow direction. The line drawn is the best fit through the plane-stress data or the data for $L \geqslant 3B$). $W = 25$ mm, $B = 1.7$ mm and $Z = 58$ mm. $w_f = 35.28 + 3.01\ L$.

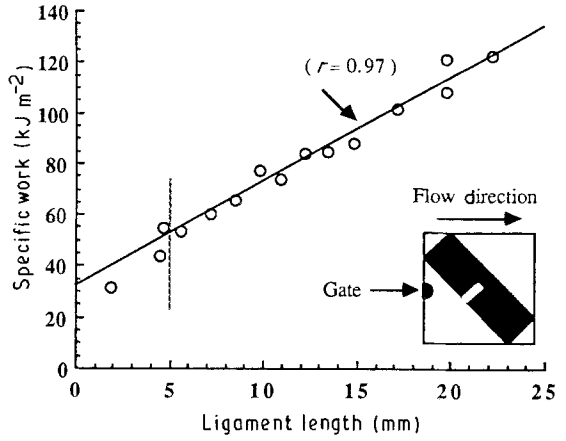

Figure 10 The total specific work of fracture, w_f, for SENT specimens as a function of ligament length, L. Crack growth is at 45° to the melt flow direction. The line drawn is the best fit through the plane-stress data or the data for $L \geqslant 3B$. $W = 25$ mm, $Z = 58$ mm and $B = 1.7$ mm. $w_f = 32.03 + 4.09\ L$.

Secondly, as we change the orientation of the initial notch with respect to the melt flow direction, the value of the specific essential work of fracture, w_e, and also the value of the specific non-essential work term changes. As shown in Table II the value of w_e is higher for a crack propagating perpendicular to the melt flow direction than when it is propagating parallel to the flow direction. However, because the monotonic tensile tests did not show any differences between either the yield stresses or the elastic moduli of samples that are cut at different angles to the direction of flow of material, the orientation dependence of w_e and the βw_p

TABLE I Fracture data for SENT specimens with cracks parallel to the melt flow direction

Position[a]	Specific essential work of fracture, w_e (kJ m^{-2})	Slope, βw_p (kJ m^{-3})	Correlation coefficient, r
A	30.54	3.27	0.945
B	25.63	3.51	0.994
C	24.71	3.54	0.942
Overall data	27.25	3.46	0.948

[a] A, B and C are as shown in Fig. 6.

TABLE II Fracture data for SENT specimens with cracks parallel, perpendicular and at 45° to the melt flow direction

Orientation (deg)	Specific essential work of fracture, w_e (kJ m^{-2})	Slope, βw_p (kJ m^{-3})	Correlation coefficient, r
0	27.25	3.46	0.948
45	32.02	4.09	0.970
90	35.28	3.01	0.954

term may be an indication that the resistance to crack propagation in polcarbonate is an anisotropic property of the material. Furthermore, the orientation dependence of the specific non-essential work term βw_p (slope of the line) indicates that the size and the shape of the plastic zone is affected by the change in the notch orientation with respect to the melt flow direction.

Finally, when w_e values were plotted against the notch orientation, Θ, a linear behaviour was observed as shown in Fig. 11. Further study is currently in progress to see if this linear behaviour truly exists.

3.1.2. Effect of the specimen geometry and size on the plane-stress essential work of fracture

To investigate any significant specimen size and specimen geometry effects on the specific essential work of fracture and the non-essential work term, tests were carried out on SENT and DENT specimens of various overall dimensions with the initial notch in the direction of the flow of the material. The results obtained are shown in Figs 12–16. From these figures the following observations could be made.

Firstly, as shown in Figs 12–14 the fracture data for the DENT specimens also give a good linear relationships between w_f and L, and the value of the specific essential work of fracture, w_e, appears to be independent of the specimen size and the geometry of the test piece. It is interesting to note that for SENT specimens with $W = 50$ mm, the specific essential work of fracture becomes independent of the ligament length (Figs 13 and 15) for reasons which are not quite clear. Furthermore, as shown in Fig. 16, altering the gauge length of the sample makes no significant effect on the measured w_e. Based on these observations, we believe that the specific essential work, w_e, is the material property for a given specimen thickness and for polycarbonate this value is approximately 28 kJ m^{-2}.

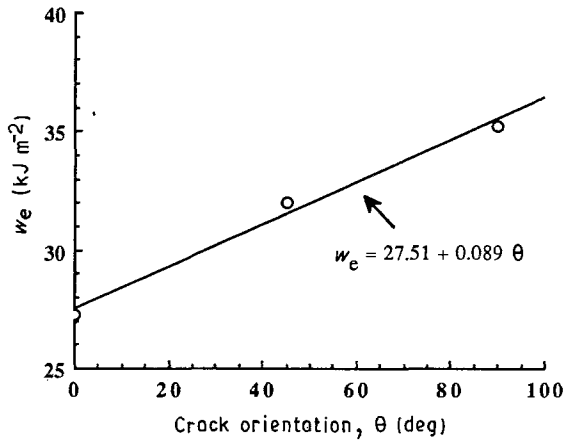

Figure 11 The specific essential work of fracture, w_e, for 1.7 mm thick SENT specimens as a function of crack orientation, W = 25 mm, Z = 58 mm. The melt flow direction is taken as 0°.

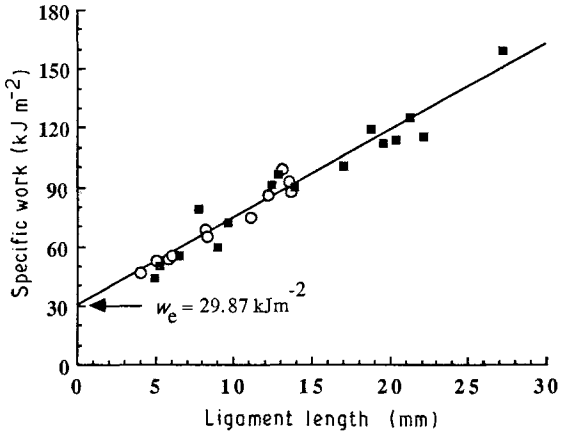

Figure 12 The specific work of fracture for (■) SENT and (○) DENT specimens as a function of the ligament length for specimen width of 35 mm, B = 1.7 mm and Z = 58 mm, and with notches parallel to the melt flow direction. The line drawn is the best fit with the equation $w_f = 29.87 + 4.44\,L$ (r = 0.942).

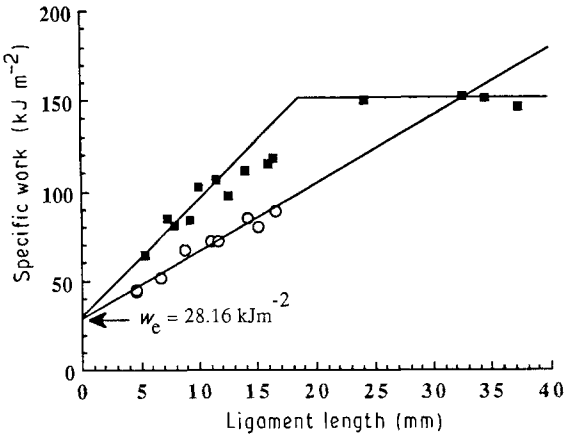

Figure 13 The specific work of fracture for (■) SENT and (○) DENT specimens as a function of the ligament length for the specimen width of 50 mm, B = 1.7 mm and Z = 58 mm, and with notches parallel to the melt flow direction.

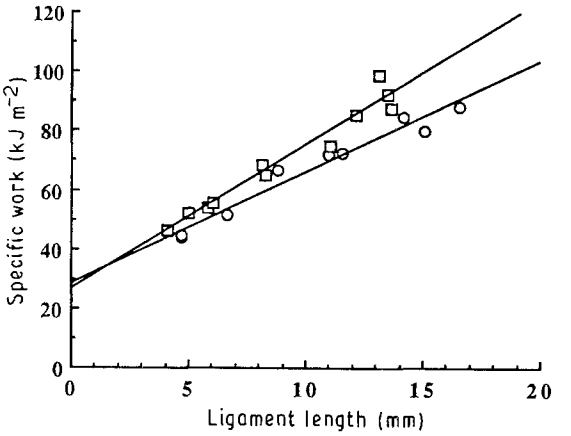

Figure 14 The specific work of fracture for DENT specimens as a function of the ligament length for specimen widths of (○) 50 mm, and (□) 35 mm, B = 1.7 mm, Z = 58 mm, with notches in the melt flow direction. For W = 50 mm: w_f = 28.26 + 3.76 L (r = 0.963). For W = 35 mm: w_f = 26.26 + 4.88 L (r = 0.958).

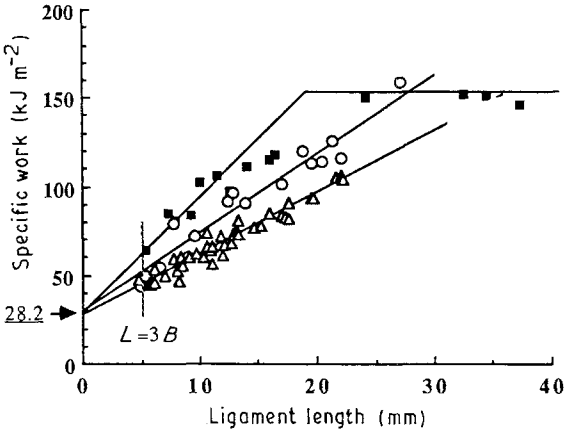

Figure 15 The specific work of fracture for SENT specimens as a function of the ligament length for specimen widths (■) 50 mm, (○) 35 mm and (△) 25 mm, B = 1.7 mm and Z = 58 mm. Notches are parallel to the melt flow direction.

Converting this specific essential work of fracture to equivalent stress intensity factor, K_c, by using the plane stress relationship $K^2 = Ew_e$ and the Young's modulus value of 2 GPa we obtain a stress intensity factor of approximately 7.48 MPa m$^{1/2}$. This value is

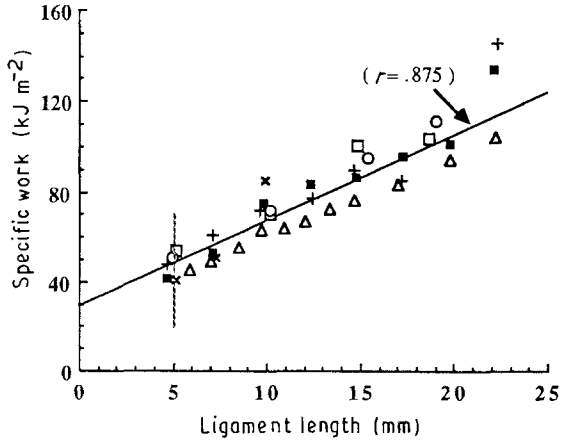

Figure 16 The specific work of fracture for SENT specimens as a function of the ligament length for several gauge length to specimen width ratios (Z/W). B = 1.7 mm, W = 25 mm. Notches are parallel to the melt flow direction. Z/W: (■) 0.72, (×) 1.12, (+) 1.52, (□) 1.92, (△) 2.32, (○) 2.72. w_f = 28.97 + 3.81 L.

higher than the value of 5.7 MPa m$^{1/2}$ obtained by Parvin and Williams using K-testing [19]. It must be noted that they used thicker samples (B = 3 mm) and therefore some differences in the K values may be expected.

Secondly, according to our results the specific non-essential work term, βw_p, could vary with the size and the geometry of the test piece. Hence, the specific non-essential work term cannot be regarded as a material property. The term βw_p depends on the shape of the outer plastic zone and, if general yielding precedes fracture initiation, as it does for polycarbonate, we expect that the shape of the outer plastic zone will be dependent on the size and the geometry of the test piece. For SENT specimens, the term βw_p appears to increase as we increase the sample width, W, as shown in Fig. 15, whereas for DENT specimens, wider specimens, gave a smaller βw_p term (Fig. 14). No significant change in the value of w_e or the value of βw_p was noted as the gauge length, Z of the test piece was changed (Fig. 16). Thus we may conclude that the specimen gauge length has no significant effect on the size of the plastic zone.

Finally, a series of tests was also performed on SENT specimens to investigate the effect of the sharpness of the initial notch on the measured values of w_e and βw_p. Specimens were consequently machine notched using 1 mm tip radius cutter. The result obtained is shown in Fig. 17 and clearly, whereas the value of w_e is not affected by the sharpness of the initial notch, the value of βw_p is significantly affected.

From the data presented so far, it is clear that the plane-stress fracture in polycarbonate is well characterized by the essential work fracture parameter w_e.

3.1.3. Plane-strain specific essential work of fracture, w_{le}, and the specific work of fracture initiation, w_i

To determine the plane-strain specific work of fracture, w_{le}, a large number of specimens was tested with

the ligament length, L, being smaller than $3B$ ($= 5$ mm). Results obtained from these tests are shown in Fig. 18. From the data it appears that w_f values in the mixed-mode stress state vary more or less linearly with the ligament length, L. To determine w_{Ie}, the best linear regression line was fitted through the data points and was extrapolated back to a zero ligament length. This extrapolation gave $w_{Ie} = 3\ \text{kJ m}^{-2}$. Converting this value to equivalent stress intensity factor we obtain a plane-strain fracture toughness value of 2.45 MPa $\text{m}^{1/2}$ in good agreement with the value of 2.24 MPa $\text{m}^{1/2}$ reported by Parvin and Williams [19]. Using the ASTM minimum specimen thickness requirement for plane-strain fracture toughness evaluation

$$B_{min} = 2.5\left(\frac{K_{Ic}}{\sigma_y}\right)^2 \quad (8)$$

and taking $K_c = 2.45$ MPa $\text{m}^{1/2}$ and $\sigma_y = 60$ MPa, we obtain $B_{min} = 4.2$ mm. Clearly, the specimen thickness used in the present study is considerably smaller than B_{min}. It would be necessary to make thicker polycarbonate samples in order to satisfy Equation 8 and thus to evaluate valid K_c values.

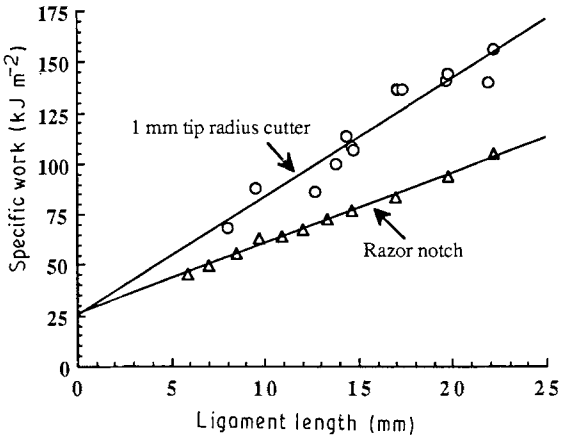

Figure 17 The specific work of fracture for SENT specimens as a function of the ligament length for two different notch tip radii and with notches parallel to the melt flow direction; $W = 25$ mm and $Z = 58$ mm. Equations of the best regression lines are: for razor notch $w_f = 25.63 + 3.51\,L$ ($r = 0.994$); for cutter $w_f = 24.36 + 5.87\,L$ ($r = 0.912$).

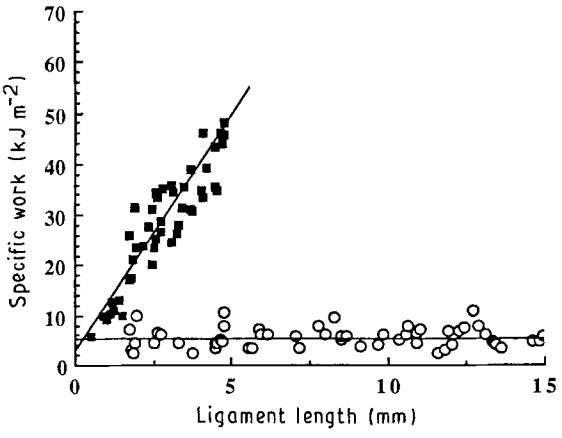

Figure 18 Plane-strain specific work of fracture, w_{Ie}, and the specific work of fracture for initiation, w_i, as a function of the ligament length. (■) Plane-stress/plane strain, (○) initiation. $w_{Ie} = 3.0\ \text{kJ m}^{-2}$, $w_i = 4.30\ \text{kJ m}^{-2}$.

For $w_{Ie} = 3\ \text{kJ m}^{-2}$ to be regarded as the true plane-strain specific essential work of fracture we may use the ASTM E-813 standard minimum thickness requirement for J_{Ic} testing, i.e.

$$B_{min} = 25\left(\frac{J_c}{\sigma_y}\right) \quad (9)$$

Replacing J_{Ic} with w_{Ie} we obtain $B_{min} = 1.25$ mm, which is smaller than the thickness of 1.7 mm used in the current study. Therefore, we conclude that the measured value of $3\ \text{kJ m}^{-2}$ is indeed the true plane strain essential work of fracture for polycarbonate.

The specific work of fracture initiation, w_i ($= W_i/LB$), is also shown in Fig. 18 as a function of ligament length. As may be seen, w_i is practically independent of ligament size and has a value of $4.3\ \text{kJ m}^{-2}$. This is somewhat smaller than the value of $6.13\ \text{kJ m}^{-2}$ determined by Singh and Parihar using the J-integral [12].

The measured w_i value ($= 4.3\ \text{kJ m}^{-2}$) is lower than the fracture propagation value of $28.0\ \text{kJ m}^{-2}$. This is because the initiation of fracture takes place at a smaller crack tip opening displacement than that for a fully propagating fracture. There is also more scatter in the measured values of w_i because of inaccuracies in determining the crack initiation point on the load–displacement diagram. In the current study, the moment when slow cracking begins was assessed visually and hence the measured values were unnecessarily influenced by human error.

The measured w_i value, on the other hand, is somewhat higher than the plane strain value, $w_{Ie} = 3\ \text{kJ m}^{-2}$. This is partly due to the inaccuracies mentioned above, and partly because the thickness for w_i is very close to the plane-strain condition given by Equation 9. Thus the measured w_i value of $3\ \text{kJ m}^{-2}$ may not be the true plane strain value even though we expect it to be very close.

Converting w_i to equivalent stress intensity factor we obtain the critical stress intensity factor of 2.93 MPa $\text{m}^{1/2}$ for fracture initiation.

4. The J-integral and the experimental results

The J-integral offers potentials for application to fracture problems where the stresses are close to or above yield. The J-integral can be interpreted as an energy release rate and in the linear elastic case $J = G$.

There are several approaches to J analysis but the two methods employed here are the direct experimental method of Landes and Begley [20] and the multi specimen R-curve method [5, 6].

4.1. Landes and Begley approach

The method is based on the definition of J as

$$J = -\frac{1}{B}\left(\frac{\partial U}{\partial a}\right) \quad (10)$$

where U is the potential energy (area under the

load–displacement curve). This method requires graphical assessment of dU/da.

Using the load–displacement curves shown in Fig. 3, curves were drawn for fixed crack length by interpolation between crack length positions marked on the load–displacement diagrams as described by Hodgkinson and Williams [21]. These were graphically integrated up to different displacements and several of these lines are shown in Fig. 19. As shown in the figure, for a given displacement, energy absorbed by a specimen decreases as the crack length increases because smaller loads are required.

For a fully yielded SENT specimen the total energy, U, is [8, 21]

$$U = B(W - a)M\sigma_y u \quad (11)$$

where M is the plastic constraint factor. Combining Equations 10 and 11

$$J = -\frac{1}{B}\left(\frac{\partial U}{\partial a}\right) = M\sigma_y u \quad (12)$$

Thus, for a fully yielded specimen, J should be linear in U and independent of crack length, a, with a slope of $M\sigma_y$. As expected, the J versus displacement, U, curves for polycarbonate are straight in the fully yielded region as shown in Fig. 20. The initial curvature in Fig. 20 is due to the linear elastic behaviour, where J is proportional to U^2 [8, 21].

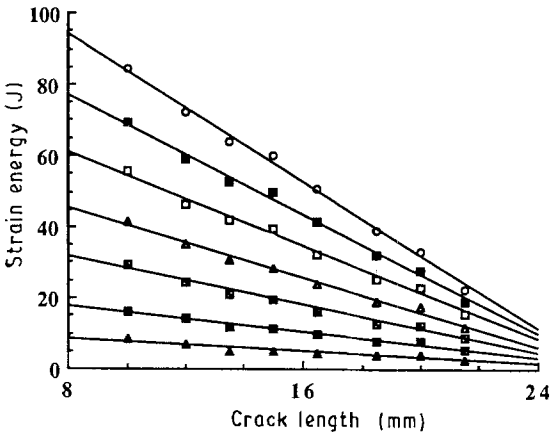

Figure 19 Energy for SENT specimens as a function of crack length at constant displacement. J is given by the slope. Notches are parallel to the melt flow direction. Specimen dimensions are W = 25 mm, B = 1.7 mm and Z = 58 mm. $U_{(mm)}$: (○) 3.2, (■) 2.8, (□) 2.4, (△) 2.0, (▨) 1.6, (⊠) 1.2 (▲) 0.8.

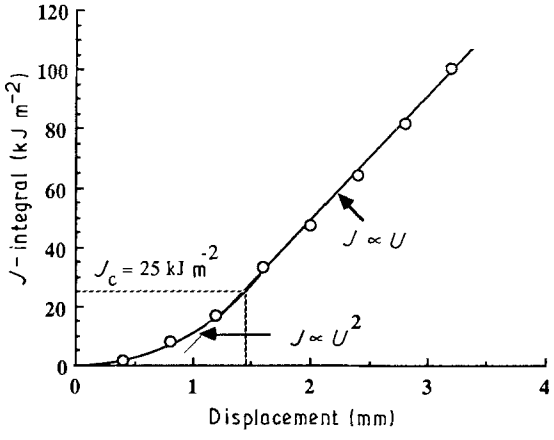

Figure 20 J as a function of displacement determined from Fig. 19.

Returning to Fig. 3, we are now able to deduce J for every point on the curves and Fig. 21 shows J versus crack extension, Δa, curves for the various initial crack lengths and for cracks growing parallel to the melt flow direction. Clearly, there is no unique J_R curve even though scatter in the data is not much. To determine the critical value of the J-integral, J_c, the best approximate line was drawn through the data points and extrapolated back to $\Delta a = 0$. The intercept on the ordinate obtained by extrapolation of a straight line gives an approximate value of 25 kJ m^{-2} for J_c. The critical value of displacement corresponding to this critical value of the J-integral is 1.45 mm. This critical value of J is much smaller than the value of 55 kJ m^{-2} reported by Singh and Parihar [12] and the value of 49.1 kJ m^{-2} reported by Ferguson *et al.* [22]. We must point out that the J_c value reported by Singh and Parihar corresponds to a crack growth of about 3 mm and is therefore expected to be higher than the true J_c value.

A similar J–Δa curve was constructed for cracks growing perpendicular and at 45° to the melt flow direction, results obtained are shown in Figs 22 and 23.

By taking the J_R curves as linear we may write

$$J = J_c + \frac{dJ}{da}\Delta a \quad (13)$$

Mai [15] used the geometric similarity argument between J and W_f to show that for SENT specimens

$$w_f = \frac{W_f}{LB} = J_c + \frac{1}{2}\frac{dJ}{da} \quad (14)$$

that is

$$w_e = J_c$$

and

$$2\beta w_p = \frac{dJ}{da} \quad (15a)$$

The comparison of estimates of dJ/da obtained from the work of fracture, $2\beta w_p$, and the J-integral for

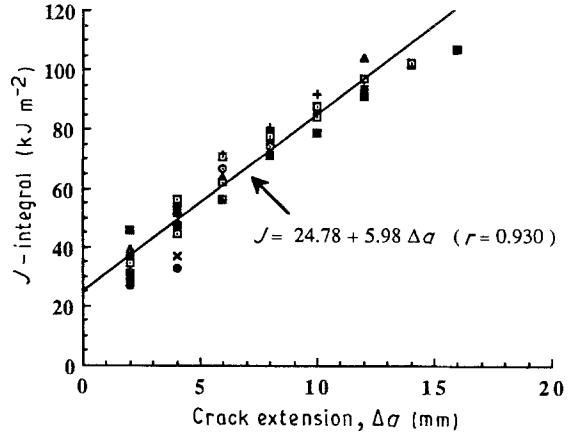

Figure 21 J versus crack extension, Δa, for various initial ligament lengths. Notches were in the melt flow direction. Lengths (mm): (■) 22.16, (△) 19.85, (□) 17.45, (◇) 14.93, (+)13.61, (⊡) 12.43, (○) 11.16, (▨) 8.67, (■) 7.36, (×) 5.95, (●) 4.67.

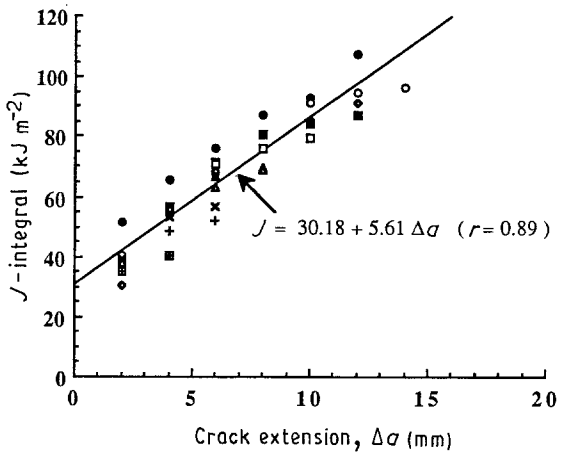

Figure 22 J versus crack extension, Δa, for various initial ligament lengths. Notches were at 45° to the melt flow direction. Lengths (mm): (●) 19.73, (○) 17.02, (◇) 14.61, (■) 13.35, (□) 12.02, (▲) 10.93, (△) 9.67, (×)8.49, (+)7.03, (⊠) 5.89.

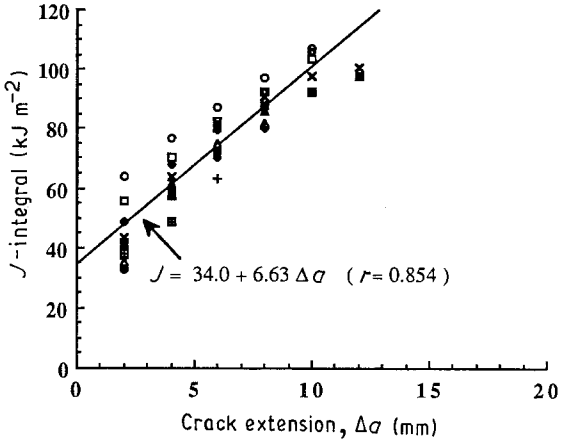

Figure 23 J versus crack extension, Δa, for various initial ligament lengths. Notches were perpendicular to the melt flow direction. Lengths (mm): (○) 22.21, (□) 19.80, (◇) 17.17, (■) 14.83, (×) 13.44, (▲) 12.23, (△) 10.91, (◆) 9.84, (+) 8.50, (⊠) 7.17, (●) 4.70.

SENT specimens is given in Table III. Clearly, the agreement between J_c and w_e is very good and that between dJ/da and $2\beta w_p$ is quite reasonable. The good agreement between these values confirms the equivalence of the two fracture parameters w_e and J_c.

4.2. Multi-specimen *R*-curve

This method is based on the definition of J as

$$J = J_e + J_p \tag{16}$$

where J_e and J_p are the elastic and plastic components of the total J value given, respectively, as

$$J_e = \frac{\eta_e U_e}{B(W - a)} \tag{17a}$$

and

$$J_p = \frac{\eta_p U_p}{B(W - a)} \tag{17b}$$

where U_e and U_p are elastic and plastic energy components, respectively, of the total energy, U_T as shown in Fig. 24. η_e and η_p are their corresponding elastic and plastic work factors. The expression for the total J may, therefore, be written as

$$J = \frac{1}{B(W - a)}(\eta_e U_e + \eta_p U_p) \tag{18}$$

The elastic work factor, η_e, can be evaluated for a given specimen geometry from the compliance or from the LEFM shape factor, $Y(a/W)$, and the plastic work factor, η_p, from the limit load analysis. For the SENT specimen geometry we have [9]

$$\eta_e = \frac{(W - a)Y^2 a}{\int Y^2 a\,da + (ZW/2)}$$

$$\eta_p = \frac{W - a}{W\alpha\{(W - a)/[W(\alpha - a/W)] + 1\}^{-1}} \tag{19}$$

where

$$\alpha = [1 - 2a/W + 2(a/W)^2]^{1/2}$$

$$Y = 1.99 - 0.41(a/W) + 18.7(a/W)^2 - 38.48(a/W)^3 + 53.84(a/W)^4$$

Z is the gauge length, a the crack length, and W the specimen width. To study the ductile fracture behaviour of polycarbonate via J_c by the multi-specimen R-curve method, identical SENT specimens with dimensions $Z = 58$ mm, $W = 25$ mm were notched to $a/W = 0.52$, in the melt flow direction. These specimens were loaded at a constant crosshead speed of 1 mm min^{-1} to various displacement values producing different amounts of crack extension, Δa, and then unloaded. After unloading, each specimen was broken open after immersion in liquid nitrogen so that the crack extension could be measured. The value of J for each specimen was determined from the area under its load versus loadline displacement curve. By substituting specimen dimensions in Equations 18 and 19 we

TABLE III Fracture data for SENT specimens

Orientation (deg)	w_e (kJ m^{-2})	$2(\beta w_p)$ (kJ m^{-3})	J_c (kJ m^{-2})	dJ/da (kJ m^{-3})
0	27.25	6.92	24.78	5.98
45	32.02	8.12	30.18	5.61
90	35.28	6.02	34.00	6.63

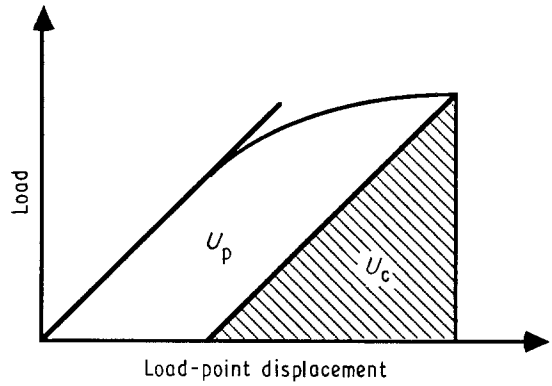

Figure 24 Schematic load versus load point displacement curve showing partitioning of elastic and plastic work.

obtain $\eta_e = \eta_p = 2.38$ and therefore Equation 18 reduces to

$$J = \frac{2.38}{B(W-a)}(U_e + U_p) = \frac{2.38\,U_T}{B(W-a)} \quad (20)$$

Thus according to Equation 20 we do not need to separate the elastic and plastic components of the total absorbed energy (total area under the load–displacement diagram).

In order to determine J_c and to construct an accurate crack growth resistance curve (J–Δa curve) several data qualifying schemes are prescribed. These include ASTM E813-81 [5] ASTM E813-87 [6], and the EGF [23] standards.

Fig. 25 shows the data for polycarbonate analysed according to ASTM E813-81. In this scheme the J–Δa points for the resistance curve must lie between two offset lines each drawn parallel to the blunting line, $J = 2\Delta a\,\sigma_y$. The minimum offset is 0.6% of the ligament length and the maximum being 6% of the ligament length. The resistance curve is then defined by the best linear regression line through the data points within these two exclusion lines as shown in Fig. 25. The intersection of the resistance curve with the blunting line gives the J_c value and according to Fig. 25 the value for polycarbonate is 36.5 kJ m^{-2}.

The ASTM E813-87 version defines the J–Δa points for the resistance curve as those data points lying between two offset lines each drawn parallel to the blunting line at 0.15 and 1.5 mm of crack extension as shown in Fig. 26. The acceptable data are then curve fitted by a power law regression line of the form

$$\ln J = \ln C + n \ln \Delta a \quad (17)$$

i.e. $J = C(\Delta a)^n$. The intersection of this power law regression line with a line parallel to the blunting line at an offset of 0.2 mm gives the value of J_c and according to Fig. 26 the value is 61.2 kJ m^{-2}. Clearly, both versions of the ASTM standard give J_c values which are much higher than the value of 24.78 kJ m^{-2} obtained by the Landes and Begley procedure. However, when the EGF [23] procedure was used, we obtained a J_c value of 24.0 kJ m^{-2} which is in excellent agreement with the Landes and Begley value. The EGF test procedure also uses the power law regression line but defines J_c as the value of J corresponding to 0.2 mm crack extension as shown in Fig. 27. The summary of the multiple specimen R-curve results is given in Table 4. It must be noted that none of the J_c values in Table IV satisfy the ASTM minimum specimen thickness requirement for plane-strain fracture, as defined by Equation 9.

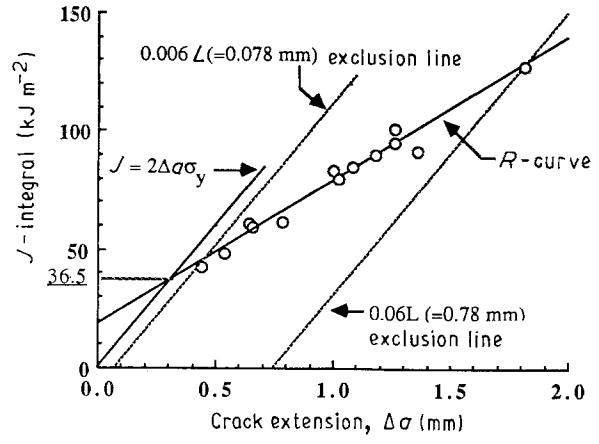

Figure 25 J versus Δa curve for SENT specimens obtained using the multiple specimen R-curve method. Analysis is according to ASTM E318-81 giving a J_c value of 36.5 kJ m^{-2}. The regression line equation is $J = 17.95 + 60.81\,\Delta a$ ($r = 0.971$).

5. Conclusions

It is shown that the plane-stress specific work of fracture, w_e, can be used to characterize the ductile fracture behaviour of polycarbonate.

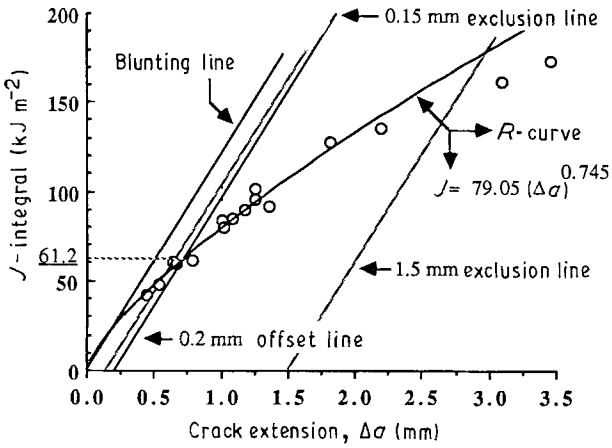

Figure 26 J versus Δa curve for SENT specimens obtained using the multiple specimen R-curve method. Analysis is according to ASTM E318-87 giving a J_c value of 61.2 kJ m^{-2}.

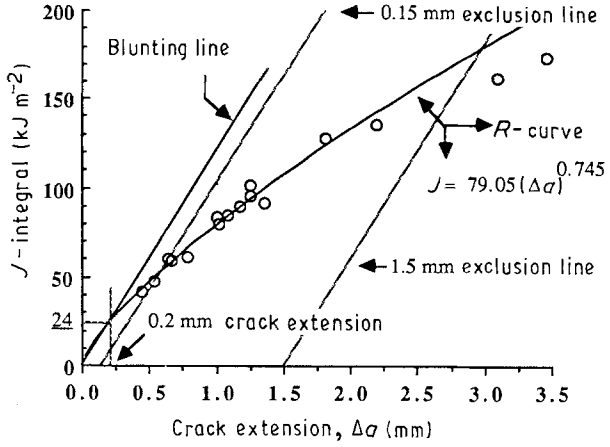

Figure 27 J versus Δa curve for SENT specimens obtained using the multiple specimen R-curve method. Analysis is according to EGF giving a J_c value of 24.0 kJ m^{-2}.

TABLE IV Multi-specimen test results

Method	J_c (kJ m^{-2})	Resistance curve	$(\Delta a)_c^a$ (mm)
ASTM E813-81	36.50	$J = 17.95 + 60.81\,\Delta a$	0.305
ASTM E813-87	61.20	$J = 79.05\,(\Delta a)^{0.745}$	0.710
EGF	24.00	$J = 79.05\,(\Delta a)^{0.745}$	0.200

[a] $(\Delta a)_c$ is the crack extension corresponding to J_c.

TABLE V Fracture data for polycarbonate (specimen thickness 1.7 mm)

	Specific essential work ($kJ\,m^{-2}$)	Stress intensity factor ($MPa\,m^{1/2}$)	J_c ($kJ\,m^{-2}$)
Plane-stress	28.00	7.48	24.78
Plane-strain	3.00	2.45	–
Initiation	4.30	2.95	–

By plotting the total specific work of fracture, w_f, against ligament length, a straight line behaviour was noted when ligament length was greater than about three times the specimen thickness (i.e. 5 mm). When ligament length was less than this value, plane-stress/plane-strain fracture was obtained.

From the results presented in this paper the following conclusions may be drawn.

1. w_e is independent of specimen width, W, specimen length, Z, and the sharpness of the initial notch.

2. w_e is independent of the specimen geometry. SENT and DENT specimens gave the same w_e value of about 28 $kJ\,m^{-2}$.

3. w_e is affected by the change in the notch orientation with respect to melt flow direction. The highest w_e value was found for specimens with the initial notch perpendicular to melt flow direction and lowest value was obtained for specimen with the initial notch parallel to the melt flow direction.

4. The specific non-essential work of fracture term, βw_p, was found to be dependent on the specimen width, specimen geometry, sharpness of the initial notch and the specimen orientation. No significant change in βw_p value was found when the specimen length was changed.

5. w_e can be identified with the value of the critical J_c integral. The agreement between w_e (= 28 $kJ\,m^{-2}$) and J_c (= 24.78 $kJ\,m^{-2}$) was found to be good when the Landes and Begley test method was employed. However, when multi-specimen R-curve method was used only the EGF treatment of the data gave a J_c value (= 24.00 $kJ\,m^{-2}$) which was comparable with w_e (28 $kJ\,m^{-2}$).

A summary of the fracture data can be found in Table V.

References

1. N. F. BROWN and J. E. SRAWLEY, ASTM STP 410 (American Society for Testing and Materials, Philadelphia, PA, 1966).
2. S. HASHEMI and J. G. WILLIAMS, *J. Mater. Sci.* **19** (1984) 3746.
3. P. L. FERNANDO and J. G. WILLIAMS, *Polym. Engng Sci.* **20** (1980) 215.
4. J. R. RICE, *J. Appl. Mech. ASME* **35** (1968) 379.
5. ASTM E813-81, 1981 Annual Book of ASTM Standards, Part 10 (American Society for Testing and Materials, Philadelphia, PA, 1981) pp. 810.
6. ASTM E813-87, 1987 Annual Book of ASTM Standards, Part 10 (American Society for Testing and Materials, Philadelphia, PA, 1987) pp. 968.
7. S. HASHEMI and J. G. WILLIAMS, *Polymer* **27** (1986) 384.
8. *Idem, Polym. Engng Sci.* **26** (1986) 760.
9. *Idem, Plastics Rubber Process. Applic.* **6** (1986) 363.
10. *Idem, J. Mater. Sci.* (1992), in press.
11. D. D. HUANG and J. G. WILLIAMS, *ibid.* **22** (1987) 2503.
12. R. K. SINGH and K. S. PARIHAR, *ibid.* **21** (1986) 3921.
13. K. B. BROBERG, *Int. J. Fract.* **4** (1968) 11.
14. B. COTTERELL and J. K. REDDEL, *ibid.* **13** (1977) 267.
15. Y. W. MAI and B. COTTERELL, *ibid.* **32** (1986) 105.
16. *Idem, J. Mater. Sci.* **15** (1980) 2296.
17. *Idem, Engng Fract. Mech.* **21** (1985) 123.
18. A. S. SALEEMI and J. A. NAIRN, *Polym. Engng Sci.* **30** (1990) 211.
19. M. PARVIN and J. G. WILLIAMS, *Int. J. Fract.* **11** (1975) 963.
20. J. D. LANDES and J. A. BEGLEY, ASTM STP 514 (American Society for Testing and Materials, Philadelphia, PA, 1972) pp. 24–39.
21. J. M. HODGKINSON and J. G. WILLIAMS, *J. Mater. Sci.* **16** (1981) 50.
22. R. J. FERGUSON, G. P. MARSHALL and J. G. WILLIAMS, *Polymer* **14** (1973) 451.
23. EGF Recommendations for Determining the Fracture Toughness for Ductile Materials (1987), private communication.

Received 30 July 1990
and accepted 6 February 1991